Carbonate versus silicate weathering in the Raikhot watershed within the High Himalayan Crystalline Series

Joel D. Blum
Carey A. Gazis*
Andrew D. Jacobson
C. Page Chamberlain
Department of Earth Sciences, Dartmouth College, Hanover, New Hampshire 03755

ABSTRACT

The major element and Sr isotope geochemistry of surface waters, bedrock, and river sands was investigated in the Raikhot watershed within the High Himalayan Crystalline Series (HHCS) in northern Pakistan. Mass-balance calculations of mineral-weathering contributions to the dissolved flux of ions from the watershed indicate that 82% of the HCO_3^- flux is derived from the weathering of carbonate minerals and only 18% is derived from silicate weathering, even though the bedrock is predominantly quartzofeldspathic gneiss and granite with only ~1% carbonate in the watershed. This study demonstrates the importance of trace amounts of bedrock carbonate in controlling the water chemistry of glacial watersheds. We suggest that the flux of Sr with a high $^{87}Sr/^{86}Sr$ ratio in the major Himalayan rivers may be derived in large part from weathering of trace amounts of calcite within the largely silicate HHCS. Models that use the flux of radiogenic Sr from the Himalayas as a proxy for silicate weathering rates may, therefore, overestimate the amount of CO_2 consumption due to silicate weathering in the Himalaya.

INTRODUCTION

The Himalayan uplift has been implicated as a major factor in the global climatic cooling of the past 40 m.y. because of enhanced silicate weathering and consequent atmospheric CO_2 drawdown (Raymo and Ruddiman, 1992). Supporting evidence for this mechanism is the dramatic increase in marine $^{87}Sr/^{86}Sr$ ratios at 40 Ma, shortly after the beginning of the Asia-India continental collision, which appears to be related to Sr inputs from major rivers draining the Himalaya (Palmer and Edmond, 1992; Edmond, 1992; Richter et al., 1992). Several workers have studied regional patterns of $^{87}Sr/^{86}Sr$ ratios in tributaries of the Ganges-Brahmaputra and Indus River systems as well as bedrock $^{87}Sr/^{86}Sr$ ratios and concluded that the major source of the highly radiogenic Sr in Himalayan rivers is weathering of silicate minerals in the HHCS (Krishnaswami et al., 1992; Pande et al., 1994; Harris, 1995). Here we report on a geochemical investigation of a single watershed within the HHCS, with the aim of elucidating the systematics of Sr release from individual minerals in the HHCS bedrock. We chose the ~200 km^2 Raikhot watershed in the western Himalaya on the north side of the Nanga Parbat massif in northern Pakistan, because it is one of the most thoroughly studied areas in the HHCS with respect to bedrock geology and geochemistry.

STUDY SITE DESCRIPTION

The Raikhot watershed has its headwaters in the glaciated cirques of the 8125 m Nanga Parbat massif and drains ~28 km to the north terminating at 1200 m in the Indus River gorge. Currently, ~20% of the watershed is covered by glacial ice, and most of the watershed area is believed to have been covered by ice during the last glacial maximum. Much of the watershed is covered by steep cliffs and talus slopes, and only ~10% of the watershed is forested. The bedrock of the Nanga Parbat massif is predominantly high-grade quartzofeldspathic biotite gneiss and schist with dikes and small plutons of anatectic biotite granite. The gneisses and schists had metasedimentary protoliths that were predominantly pelitic sedimentary rocks. Minor amounts of calcareous sedimentary rocks and basaltic dikes give rise to thin layers and lenses of marble as well as calc-silicate and amphibolite schist, which together make up only a small (~1%) proportion of the outcrop exposure area. Bedrock mapping has been carried out in the ~50% of the watershed that is both ice free and accessible (e.g., Zeitler et al., 1993; Chamberlain et al., 1995), and observations of rock types in glacial moraines confirm that the unmapped parts of the watershed have bedrock similar to that of the well-mapped areas.

Although the protolith ages of these rocks are ca. 1.8 Ga, they have been metamorphosed and rapidly uplifted within the past 10 m.y. (e.g., Zeitler et al., 1993). As a result of this recent metamorphism, biotite and feldspars have young and nearly concordant Ar-Ar and Rb-Sr ages (e.g., Zeitler et al., 1993; Gazis et al., 1995). The bedrock protolith and geologic history of this area are believed to be generally representative of the entire HHCS, which extends over 2000 km across the length of the Himalayan Mountain Range and dominates the geology of the steep southern slopes that are subjected to rapid physical erosion during the monsoon season (Harris, 1995). The ages of rocks currently at the surface in the Nanga Parbat region are, however, younger than those in much of the HHCS, which underwent peak metamorphism and granitic intrusion at 10 to 40 Ma (e.g., LeFort et al., 1987).

SAMPLING AND ANALYTICAL METHODS

Samples for analysis were taken of rainwater, snow, clear streams, Raikhot River water (which has abundant suspended glacial flour), Raikhot riverbed sand, bedrock from outcrops, and bedrock boulders collected on the surface of the Raikhot Glacier (Tables 1 and 2). All water samples were collected in acid-washed polyethylene bottles. Stream and river samples were filtered in the field through acid-washed 0.45 μm polypropylene filters, and at each sampling site an unfiltered sample was also collected and filtered 6 to 12 months later. Gran titrations were carried out in the field to determine carbonate alkalinity, and SO_4^{2-}, NO_3^- and Cl^- concentrations were determined in the laboratory by ion chromatography. NO_3^- and Cl^- concentrations are negligible, and the ratio of HCO_3^-/SO_4^{2-} varies from ~10 in the Raikhot River to ~4 in the clear streams.

Rock samples containing calcite were leached for 1 h in 4*N* acetic acid to dissolve calcite for analysis. Silicate rock samples were digested with a $LiBO_2$ flux for elemental analysis and with hydrofluoric and perchloric acids for Sr isotope analysis. A sample of Raikhot riverbed sand (believed to be representative of unweathered bedrock from the watershed) was collected below the glacier terminus. It was sieved to <2 mm and split into two representative subsamples, one of which was left uncrushed and the other of which was crushed to a fine powder. Each of these two subsamples was first leached in 4*N* acetic acid, which was assumed to remove for measurement the average carbonate fraction present in the watershed, and then the remaining silicate material was digested in hydrofluoric and perchloric acids to allow analysis of the average silicate fraction.

Concentrations of major elements and Sr were measured to an accuracy of ±10% by inductively coupled plasma optical emission spectrometry, and Ca and Sr were measured on rain and snow by inductively coupled plasma mass spectrometry. Sr was separated with Eichrom Sr-specific resin; total procedural blanks were <70 pg of Sr. $^{87}Sr/^{86}Sr$ ratios were measured on a Finnigan MAT 262 thermal-ionization mass spectrometer to a preci-

---

*Present address: Department of Geology, Central Washington University, Ellensburg, Washington 98926.

sion of at least ±0.000 020 (2σ). The ^{86}Sr/^{88}Sr ratio was normalized to 0.1194 and analyses of the NBS-987 standard yielded a mean ^{87}Sr/^{86}Sr ratio of 0.710 243 ± 0.000 022 (2σ, $n = 44$).

RESULTS AND DISCUSSION

Major Elements

The most abundant minerals in the bedrock of the watershed are quartz, plagioclase, K-feldspar, and biotite. Calcite is present in only minor abundance but is highly reactive in glacial environments (Anderson et al., 1997). In recently glaciated temperate environments, plagioclase and K-feldspar are assumed to weather to kaolinite, and biotite to vermiculite (or hydrobiotite) (e.g., Blum et al., 1994; Blum and Erel, 1997). The dissolved weathering products of calcite, plagioclase, K-feldspar, and biotite are plotted in a ternary diagram with apices (Na + K), (Si), and (Ca + Mg) (Fig. 1). The compositions of stream waters and Raikhot River samples are also plotted and form a cluster that lies in a triangle defined by the weathering reactions for plagioclase, biotite, and calcite (Fig. 1). Laboratory-filtered Raikhot River samples plot closer to calcite, reflecting dissolution of suspended calcite in the sample bottles during transport and storage.

TABLE 1. ANALYTICAL RESULTS FOR WATER SAMPLES

Sample number	Filtered	Notes	Ca (μmol/L)	K (μmol/L)	Mg (μmol/L)	Na (μmol/L)	Si (μmol/L)	Sr (nmol/L)	^{87}Sr/^{86}Sr	% HCO$_3^-$ from carb*
Raikhot River										
96W5	yes		257	53	43	38	83	103	0.770 649	84.3
	no		730	77	57	46	112	379	0.743 101	91.5
	no		740	70	52	28	89	375	0.734 718	93.7
96W15	yes		358	64	57	49	127	171	0.766 901	85.3
	no		672	79	66	58	106	425	0.750 599	89.6
95W14	yes		217	50	56	34	53	101	0.774 488	84.3
	no		445	51	42	36	67	296	0.749 649	90.6
Clear Streams		Bedrock								
96W1	yes	gneiss	325	52	83	100	141	108	0.796 121	77.3
	no		387	57	93	108	147	186	0.795 920	78.8
96W2	yes	gneiss	348	51	97	84	140	107	0.793 204	81.6
	no		406	56	109	95	144	186	0.793 036	82
96W4	yes	gneiss	346	51	96	83	138	107		81.6
	no		416	56	109	91	143	188		82.7
96W14	yes	gneiss	188	47	41	56	105	67		75.4
	no		234	58	48	64	103	142		76.4
95W15	yes	gneiss	441	89	92	136	194	182		75.1
	no		489	96	97	144	194	271		75.8
95W4	yes	gneiss	423	41	47	112	175	132		79
	no		482	47	52	115	176	180		80.5
95W3	yes	granite	699	78	89	147	178	254	0.809 121	81.9
	no		714	74	89	144	171	257	0.806 164	82.6
95W5	yes	granite	387	47	53	125	215	108	0.841 356	75.4
	no		435	55	59	131	194	177	0.841 426	76.4
95W7	yes	moraine	512	28	64	65	151	352	0.743 314	89.6
	no		576	36	70	72	138	415	0.743 411	89.3

* Calculated percent of HCO$_3^-$ in water from carbonate dissolution; see text for explanation.

TABLE 2. ANALYTICAL RESULTS FOR ROCK LEACHATES AND DIGESTS

Sample number	Notes	Ca (μmol/g)	K (μmol/g)	Mg (μmol/g)	Na (μmol/g)	Si (μmol/g)	Sr (nmol/g)	^{87}Sr/^{86}Sr
Leachates - 4*N* acetic acid								
P1590	gneiss	4419	1.73	7.31	1.46	6.03	2021	0.734 435
P198a92	gneiss	4001	2.33	3.48	3.41	8.00	2466	0.722 258
P198b92	gneiss	956	7.07	10.34	2.49	6.96	444	0.719 899
PT203a	gneiss	4168	2.49	6.77	2.90	9.27	2399	0.725 539
96R6a	gneiss	584	3.51	2.44	5.01	6.64	216	0.823 624
96R6b	gneiss	443	3.95	7.42	6.58	12.72	205	0.741 695
96R6c	gneiss	4054	3.67	7.59	2.29	5.82	3544	0.718 559
96R6d	gneiss	1102	3.13	3.64	3.89	17.74	574	0.726 148
96R6e	gneiss	169	3.40	2.54	4.58	8.19	81	0.755 181
96S15	river sand*	125	16.51	20.30	9.85	6.08	97	0.743 220
96S15	river sand†	93	3.37	11.58	1.94	2.54	66	0.723 124
Silicate digests - hydrofluoric and perchloric acid								
96S15§	river sand*	323	801	193	841	--------	1530	0.866 939
96S15§	river sand†	305	885	185	888	12544	1597	0.861 837
P44a90	granite	235	1136	20	1136	12381	719	0.887 760
P12a90	gneiss	399	1384	298	732	11250	1792	0.823 580
95R4	gneiss	414	1499	424	678	10934	1849	0.818 230
95R5	gneiss	52	2278	754	161	9636	713	0.883 870

*Crushed

†Uncrushed

§Total digest of samples after 4*N* acetic acid leach.

A mass-balance calculation was performed to quantify the proportions of each of the important bedrock minerals that weathered to yield each water composition. This six-step calculation—based on the stoichiometry of the assumed weathering reactions—also allowed the estimation of the proportion of HCO$_3^-$ that was derived from silicate versus carbonate weathering (Table 1). *(1) Assessment of the importance of atmospheric input to stream- and river-water compositions.* Two rainwater and five snow-pack samples were collected and analyzed from the region. Concentrations were very low (<2.5 μmol/L for Ca, K, Mg, Na, and Si; <5 nmol/L for Sr); thus atmospheric correction is unnecessary, and omitting it does not affect any of the results of this investigation. *(2) Attributing of all Na in stream and river waters to the weathering of albite to kaolinite.* According to this reaction when balanced, 2 mol of Si and 1 mol of HCO$_3^-$ are also subtracted for each mole of Na. *(3) Attributing of Ca in proportion to the Ca/Na ratio of plagioclase to the weathering of anorthite to kaolinite.* We use the Ca/Na ratio of 0.38 measured in the silicate fraction of the riverbed sand as an estimate because plagioclase dominates the Ca and Na budgets of the silicate fraction. According to this reaction, 2 mol of HCO$_3^-$ are subtracted for each mole of Ca. *(4) Attributing any remaining Si to the weathering of orthoclase to kaolinite.* According to this reaction, 0.5 mol of K and 0.5 mol of HCO$_3^-$ are subtracted for each mole of this Si. *(5) Attributing the remaining K to the weathering of biotite to vermiculite.* According to this reaction 1 mol of HCO$_3^-$ is subtracted for each mole of K. *(6) Attributing excess Ca and Mg to carbonate dissolution.* According to this reaction, 2 mol of HCO$_3^-$ are subtracted for each mol of Ca + Mg.

For the field-filtered Raikhot River samples, the above mass-balance calculation yields an estimate of the relative amounts of weathering of bedrock minerals as follows: 14% plagioclase, 2% orthoclase, 11% biotite, and 73% carbonate. This estimate corresponds to a riverine HCO$_3^-$ flux that is 18% derived from silicate and 82% derived from carbonate weathering reactions. Separate analyses of the carbonate and silicate fractions of the riverbed sand indicate that only 1.0 wt% of the sediment load is carbonate (Table 2). The calculated percentages of weathering of bedrock minerals for the average quartzofeldspathic gneiss and granite bedrock stream waters were: 24% plagioclase, <1% orthoclase, 12% biotite, and 64% carbonate. High proportions of HCO$_3^-$ are also derived from carbonate (68%–78%) in the stream waters known to drain exclusively quartzofeldspathic gneiss and granite bedrock.

Ca/Sr Ratios and Sr Isotope Systematics

The Ca/(1000Sr) ratios of silicate rocks (gneiss and granite) range from 0.07 to 0.4, whereas marble layers range from 1 to 2. ^{87}Sr/^{86}Sr ratios of the silicate rocks (and all their constituent minerals; Gazis et al., 1995) range between 0.82 and 0.89, whereas marble layers range from 0.71 to 0.73. The riverbed sand silicate and carbonate samples are taken to be reliable average values for silicate and carbonate in the watershed. Surprisingly, in plots of both Ca/(1000Sr) versus ^{87}Sr/^{86}Sr (Fig. 2) and Ca/(1000Sr) versus the percent of HCO$_3^-$ derived from dissolution of carbonate (Fig. 3), river and stream-water samples from the watershed do not plot on a mixing line between the average silicates and marbles. In both Figures 2 and 3, water samples plot within a triangle defined by silicate, marble, and an additional weathering end member, which must have a Ca/(1000Sr) ratio over 4.5 and ^{87}Sr/^{86}Sr ratio over 0.82 to satisfy mixing relationships in Figure 2, and also must be calcite to satisfy mixing relationships in Figure 3.

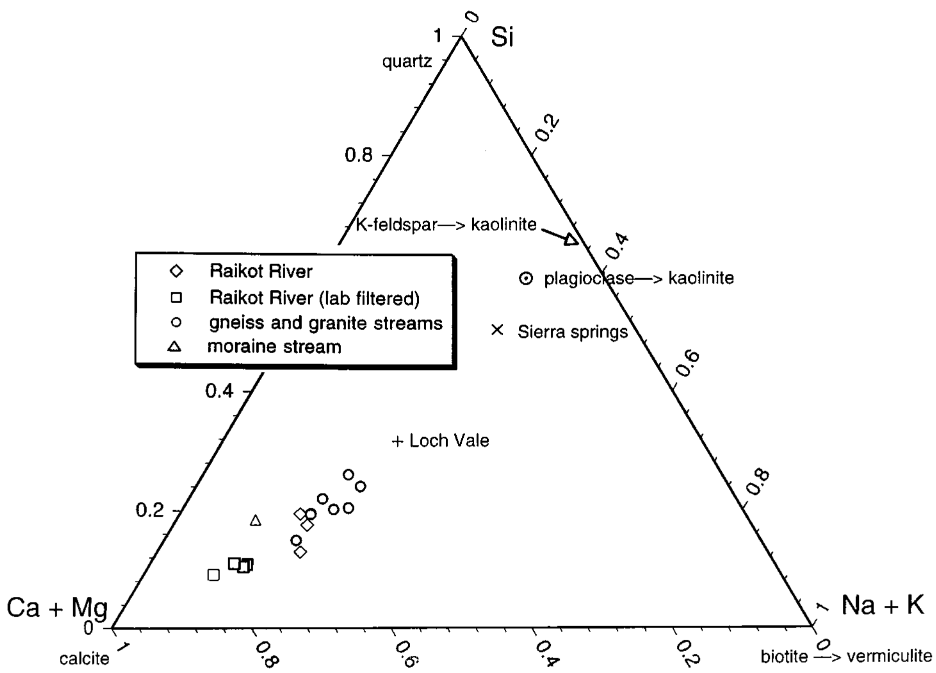

Figure 1. Ternary plot showing proportions of major elements released by weathering reactions. Quartz, calcite, and biotite dissolved weathering products plot at the three apices, and K-feldspar weathering products plot on edge of triangle. Position of plagioclase weathering products depends on Ca/Na ratio of plagioclase; average for watershed is shown as open circle with centered dot. Average water compositions of Sierra Nevada springs and Loch Vale, Colorado, watershed (Mast et al., 1990) are also shown as examples of water compositions that result from "normal" granitic weathering, and weathering of gneiss containing trace calcite, respectively. Raikhot watershed water analyses are shown as open symbols that are identified on plot.

Leachates of marble bands and the carbonate fraction of calc-silicate gneiss samples containing calcite range from Ca/(1000Sr) and ^{87}Sr/^{86}Sr values similar to the average defined by the riverbed sand up to values approaching those appropriate for the additional end member (Fig. 2). The varying degrees of Sr isotopic equilibration of these calcites with silicates are consistent with other studies that have found varying levels of Sr isotope equilibration between silicate and carbonate bands in high-grade metamorphic rocks (Bickle et al., 1995). Traces of finely disseminated calcite veins and blebs are also found commonly in thin sections of quartzofeldspathic gneiss and granite and associated with quartz veins in the watershed (Craw et al., 1994; this study). Although we have not measured it directly, we infer that this vein calcite end member has a Ca/(1000Sr) of >4.5 (Fig. 2), which is higher than that observed for most

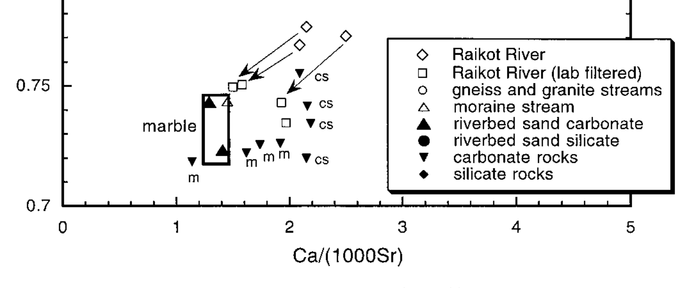

Figure 2. Ca/(1000Sr) ratio plotted versus ^{87}Sr/^{86}Sr for water samples, rocks, and rock leachates. Arrows connect field-filtered and laboratory-filtered Raikhot River samples. Carbonate rock analyses are designated "m" for calcite from massive marble bands and "cs" for calcite from finely laminated calc-silicate-rich rocks. Vein-calcite end member is inferred on the basis of mixing relationships.

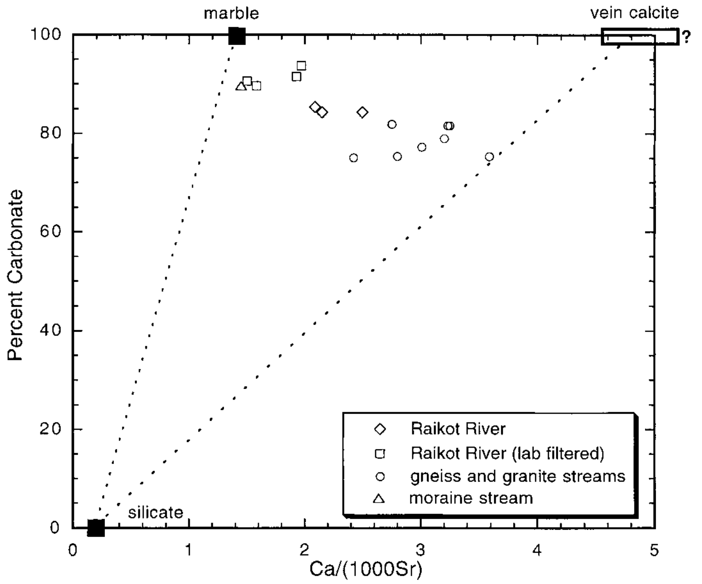

Figure 3. Ca/(1000Sr) ratio plotted versus calculated percent of HCO$_3^-$ in waters derived from carbonate dissolution, as described in text. Average marble and silicate rock values (solid squares) are estimated from Raikhot riverbed sand analyses. Vein-calcite end member is inferred on basis of mixing relationships.

marbles, but within the range observed in other studies of vein calcites in granites and gneisses (e.g., Komor, 1995; Clauer et al., 1989). We infer that this finely disseminated calcite has equilibrated isotopically with the silicates and thus has a $^{87}Sr/^{86}Sr$ ratio of ~0.86 (Fig. 2). We hypothesize that the pervasive young metamorphism and hydrothermal fluid flow in this region caused partial equilibration of marble bands with quartzofeldspathic gneisses, resulting in progressive increases in the Ca/Sr and $^{87}Sr/^{86}Sr$ ratios of metasedimentary carbonates and precipitation of disseminated calcite. We conclude that the gneiss and granite-draining streams with the highest Ca/Sr and $^{87}Sr/^{86}Sr$ ratios represent dissolution of ~75% vein calcite and ~25% silicate minerals, which when mixed with marble defines the composition of all the waters in the watershed (Fig. 3).

CONCLUSIONS AND IMPLICATIONS

We conclude that even in the predominantly silicate Raikhot watershed of the HHCS, the cation and HCO_3^- flux is predominantly derived from the dissolution of a small amount of calcite (~1%) found in thin layers of metasedimentary rocks and finely disseminated as veins within quartzofeldspathic gneisses and granites. If the results from this single watershed can be extrapolated to the entire HHCS (and we think that they can, although the extrapolation remains to be demonstrated), then the implication of our finding is that the flux of highly radiogenic Sr to the oceans related to the Himalayan uplift was predominantly derived from dissolution of carbonate minerals, which has no net effect on rates of atmospheric CO_2 consumption (e.g., Berner, 1994). Thus, models using the flux of radiogenic Sr from the Himalayas that assume this flux is due to silicate weathering may overestimate the amount of CO_2 consumption due to silicate weathering in the Himalayas.

Our conclusions are generally consistent with large-scale regional studies of the Ganges-Brahmaputra and Indus Rivers which have suggested that about two-thirds of the dissolved cations are derived from carbonate weathering and about one-third from silicate weathering (Krishnaswami et al., 1992), although we add the observation that carbonate weathering dominates even in the predominantly silicate HHCS. Our work supports the speculation of Palmer and Edmond (1992) that the high Sr flux and $^{87}Sr/^{86}Sr$ ratio of major Himalayan rivers are likely controlled by carbonates with high $^{87}Sr/^{86}Sr$ ratios that had reequilibrated with silicates having high $^{87}Sr/^{86}Sr$ ratios during metamorphism. We find that the precipitation of disseminated calcite by hydrothermal fluids plays a much more important role than previously recognized.

Quade et al. (1997) recently argued that metamorphosed carbonate rock has played a role in the high $^{87}Sr/^{86}Sr$ ratios of the Himalayan rivers by studying paleosols from the Himalayan foreland basin. We concur with this conclusion and add the finding that weathering of vein calcite in the highland catchments contributes an additional source of carbonate-derived Sr with even higher $^{87}Sr/^{86}Sr$ ratios. We also support the conclusion that the geologic record of $^{87}Sr/^{86}Sr$ variation in Himalayan rivers through time (Derry and France-Lanord, 1996; Quade et al., 1997) cannot be used to directly calculate the amount of CO_2 consumption by silicate weathering in the Himalaya (Quade et al., 1997). Instead, we find that weathering reactions releasing the high $^{87}Sr/^{86}Sr$ flux of dissolved Sr from the HHCS derive only ~18% of their HCO_3^- from silicate weathering.

ACKNOWLEDGMENTS

We thank Jay Quade for a helpful review, and M. Poage, D. Leone, C. Blum, and A. Klaue for assistance in the field and laboratory. This work was funded by National Science Foundation grant EAR-9418154 as part of the Nanga Parbat Continental Dynamics Project.

REFERENCES CITED

Anderson, S. P., Drever, J. I., and Humphrey, N. F., 1997, Chemical weathering in glacial environments: Geology, v. 25, p. 399–402.

Berner, R. A., 1994, GEOCARB II: A revised model for atmospheric CO_2 over Phanerozoic time: American Journal of Science, v. 294, p. 56–91.

Bickle, M. J., Chapman, H. J., Wickham, S. M., and Peters, M. T., 1995, Strontium and oxygen isotope profiles across marble-silicate contacts, Lizzies Basin, East Humboldt Range, Nevada: Constraints on metamorphic permeability contrasts and fluid flow: Contributions to Mineralogy and Petrology, v. 121, p. 400–413.

Blum, J. D., and Erel, Y., 1997, Rb-Sr isotope systematics of a granitic soil chronosequence: The importance of biotite weathering: Geochimica et Cosmochimica Acta, v. 61, p. 3193–3204.

Blum, J. D., Erel, Y., and Brown, K., 1994, $^{87}Sr/^{86}Sr$ ratios of Sierra Nevada stream waters: Implications for relative mineral weathering rates: Geochimica et Cosmochimica Acta, v. 58, p. 5019–5025.

Clauer, N., Frape, S. K., and Fritz, B., 1989, Calcite veins of the Stripa granite (Sweden) as records of the origin of the groundwaters and their interactions with the granitic body: Geochimica et Cosmochimica Acta, v. 53, p. 1777–1781.

Chamberlain, C. P., Zeitler, P. K., Barnett, D. E., Winslow, D., Poulson, S. R., Leahy, T., and Hammer, J. E., 1995, Active hydrothermal systems during the recent uplift of Nanga Parbat, Pakistan Himalaya: Journal of Geophysical Research, v. 100, p. 439–453.

Craw, D., Koons, P. O., Winslow, D., Chamberlain, C. P., and Zeitler, P., 1994, Boiling fluids in a region of rapid uplift, Nanga Parbat Massif, Pakistan: Earth and Planetary Science Letters, v. 128, p. 169–182.

Derry, L. A., and France-Lanord, C., 1996, Neogene Himalayan weathering history and river $^{87}Sr/^{86}Sr$: Impact on the marine Sr record: Earth and Planetary Science Letters, v. 142, p. 59–74.

Edmond, J. M., 1992, Himalayan tectonics, weathering processes, and the strontium isotope record in marine limestones: Science, v. 258, p. 1594-1597.

Garrels, R. M., and Mackenzie, F. T., 1967, Origin of the chemical composition of some springs and lakes, *in* Gould, R. F., ed., Equilibrium concepts in natural water systems: Washington, D.C., American Chemical Society, Advances in Chemistry Series, v. 67, p. 222–242.

Gazis, C. A., Blum, J. D., and Chamberlain, C. P., 1995, The effect of hydrothermal activity on the Sr isotope systematics of gneisses from the Nanga Parbat-Haramosh Massif (Northwest Himalaya, Pakistan): Eos (Transactions, American Geophysical Union), v. 76, p. F704.

Harris, N., 1995, Significance of weathering Himalayan metasedimentary rocks and leucogranites for the Sr isotope evolution of seawater during the early Miocene: Geology, v. 23, p. 795–798.

Komor, S. C., 1995, Chemistry and petrography of calcite in the KTB pilot borehole, Bavarian Oberpfalz, Germany: Chemical Geology, v. 124, p. 199–215.

Krishnaswami, S., Trivedi, J. R., Sarin, M. M., Ramesh, R., and Sharma, K. K., 1992, Strontium isotopes and rubidium in the Ganga-Brahmaputra river system: Weathering in the Himalaya, fluxes to the Bay of Bengal and contributions to the evolution of oceanic $^{87}Sr/^{86}Sr$: Earth and Planetary Science Letters, v. 109, p. 243–253.

LeFort, P., Cuney, C., Deniel, C., France-Lanord, C., Sheppard, S. M. F., Upreti, B. N., and Vidal, P., 1987, Crustal generation of the Himalayan leucogranites: Tectonophysics, v. 134, p. 39–57.

Mast, M. A., Drever, J. I., and Baron, J., 1990, Chemical weathering in the Loch Vale watershed, Rocky Mountain National Park, Colorado: Water Resources Research, v. 26, p. 2971–2978.

Palmer, M. R., and Edmond, J. M., 1992, Controls over the strontium isotope composition of river water: Geochimica et Cosmochimica Acta, v. 56, p. 2099–2111.

Pande, K., Sarin, M. M., Trivedi, J. R., Krishnaswami, S., and Sharma, K. K., 1994, The Indus River system (India-Pakistan): Major-ion chemistry, uranium and strontium isotopes: Chemical Geology, v. 116, p. 245–259.

Quade, J., Roe, L., DeCelles, P. G., and Ojha, T. P., 1997, The late Neogene $^{87}Sr/^{86}Sr$ record of lowland Himalayan rivers: Science, v. 276, p. 1828–1831.

Raymo, M. E., and Ruddiman, W. F., 1992, Tectonic forcing of late Cenozoic climate: Nature, v. 359, p. 117–122.

Richter, F. M., Rowley, D. B., and DePaolo, D. J., 1992, Sr isotope evolution of seawater: The role of tectonics: Earth and Planetary Science Letters, v. 109, p. 11–23.

Zeitler, P. K., Chamberlain, C. P., and Smith, H. A., 1993, Synchronous anatexis, metamorphism, and rapid denudation at Nanga Parbat (Pakistan Himalaya): Geology, v. 21, p. 347–350.

Manuscript received October 16, 1997
Revised manuscript received February 4, 1998
Manuscript accepted February 17, 1998